Efficient Computation of SAR and Temperature Rise Distributions in a Human Head at Wide Range of Frequencies Due to 5G RF Field Exposure

Fatih Kaburcuk [1] and Atef Z. Elsherbeni [2]

[1] Electrical and Electronic Engineering Department
Erzurum Technical University, Erzurum, 25700, Turkey
fkaburcu@syr.edu – fatih.kaburcuk@erzurum.edu.tr

[2] Electrical Engineering Department
Colorado School of Mines, Golden, CO, 80401, USA
aelsherb@mines.edu

Abstract ─ In this paper, the effects of radio frequency electromagnetic fields produced by base stations on a human head are investigated with the aid of a multiphysics model at multiple frequencies using a single simulation. This multiphysics model is based on integrating the Debye model of human head dispersive tissues parameters into the finite-difference time-domain method by using the auxiliary differential equation approach and then calculating the specific absorption rate and temperature rise distributions in the head with the use of bioheat equation. The effects of frequency and incident angle of radio frequency electromagnetic fields on the specific absorption rate and temperature rise distributions in the head are analyzed.

Index Terms ─ Biologic effects of electromagnetic radiation, dispersive head, FDTD method, multiphysics model, specific absorption rate, temperature rise.

I. INTRODUCTION

In recent years, the number of the base stations mounted on towers and rooftops has increased with the use of mobile phones. As a consequence, it is important to consider the possible harmful effects on human tissues due to radio frequency (RF) electromagnetic fields by the base station antennas. The maximum permissible exposure limits from the base station antenna are determined for occupational and general public exposures. For the occupational exposure, RF worker needs to work very close to the base station antennas, whereas, for the public exposure, people received RF fields stay far away from the base station antennas. Many international protection organizations [1-3] have presented safety standards for limiting RF exposure. These standards have basic restriction and reference levels for occupational and public exposures which are dependent on the frequency ranges.

The thermal effect of the RF electromagnetic fields on a human head has been studied due to far-field [4-8] and near-field exposures [8-12] from different types of the antennas using the traditional finite-difference time-domain (FDTD) method. Additionally, several researchers have investigated the thermal effect on a human eye, one of the most sensitive organs in the human head for the RF field exposure, due to far-field exposure [13-16] and near-field exposure [16-18]. In the previous works [4-18], temperature rise and specific absorption rate (SAR) distributions in the human head or eye were calculated at only one frequency of interest in a single simulation because of frequency dependent of the electromagnetic properties of the biological tissues. Therefore, these distributions cannot be calculated for multiple frequencies of interest in a single simulation. A multiphysics model based on the FDTD method proposed in [19] allows to calculate these distributions at multiple frequencies in the human head due to a wideband antenna using a single FDTD simulation.

During the last few years, a fifth generation (5G) mobile communication has gained enormous popularity and extensive research interest. Its possible effects on a human head are not studied significantly. In this paper, the interaction between a human head and the RF electromagnetic fields due to the 5G base stations for the occupational and public exposures are investigated using the multiphysics model. Thus, SAR and temperature rise distributions in the head are obtained at possible operating frequencies of the 5G base stations using a single simulation. In this investigation, the frequency ranges of the RF electromagnetic fields radiated by the 5G base stations are 3.4-3.8 GHz and 4.4-4.9 GHz.

In the multiphysics model, the Debye model is integrated into the FDTD method using the auxiliary differential equation (ADE) as presented in [20], then the SAR and temperature rise with the use of Pennes bioheat equation [21] are calculated. In the Debye model, the three-term Debye coefficients (the relative permittivity

Submitted On: June 12, 2018
Accepted On: November 4, 2018

of medium at infinite frequencies, the static relative permittivity, and the relaxation time) calculated and tabulated in [22] are used as the dispersive EM properties of the human head tissues for a wide range of frequencies (500 MHz to 20 GHz).

In this paper, a realistic head model [23] under RF electromagnetic fields exposure due to the 5G base stations is analyzed to prove the validity of the multiphysics model. The SAR and temperature rise distributions in the head at multiple frequencies 3.4, 3.8, 4.4, and 4.9 GHz are calculated using the multiphysics model in a single simulation as well as using the traditional FDTD method in multiple simulations. The effect of incident angle of the RF fields on the SAR and temperature rise distributions in the head is also investigated.

II. MULTIPHYSICS MODEL

A. Human head model with dispersive tissues

A three dimensional realistic head model generated in [23] is used in this work. The head model used here consists of eight tissues (skin, muscle, bone, blood, fat, lens, and white and grey matter) and 172(width)× 208(depth)×240(height) cubic cells. In order to ensure the numerical stability in the FDTD method, the cell size should be less than $\lambda_{\min}/10$, where $\lambda_{\min}$ is the wavelength of the highest frequency in the head model. Therefore, the head model is divided into 0.9 mm cells in all directions to satisfy this criterion.

The complex relative permittivity $\left(\varepsilon_r^*(\omega)\right)$ for the three-term Debye coefficients is defined [22] as:

$$\varepsilon_r^*(\omega) = \varepsilon_\infty + \sum_{k=1}^{3} \frac{\Delta\varepsilon_k}{1 + j\omega\tau_k}. \tag{1}$$

where $\Delta\varepsilon_k = \varepsilon_{s_k} - \varepsilon_\infty$, ε_∞ is the relative permittivity at infinite frequencies, ε_{s_k} and τ_k are the static relative permittivity and the relaxation time constant of *k*th term, respectively. They were obtained using a numerical technique developed in [22] for the frequency range 500 MHz to 20 GHz.

B. FDTD method and incident plane wave

The RF electromagnetic fields radiated by the 5G base stations are considered as far-field sources generated somewhere outside of the FDTD problem domain. The FDTD problem domain involved the head model is illuminated by the incident plane wave produced from these sources. The power density of the incident plane wave are set to 50 W/m^2 and 10 W/m^2 which are maximum permissible exposure limits for occupational and public exposures [1-2], respectively. The incident plane wave is a Gaussian waveform containing each frequency of interest. The total-field/scattered-field formulation [20] used here generates the incident plane wave in the FDTD problem domain. The convolution perfect matching layer (CPML) [20] as an absorbing boundary is applied at the borders to truncate the FDTD problem domain.

C. SAR calculation

The RF energy absorbed per unit mass of biological tissue is defined as SAR. The spatial peak SAR value over any 1g tissue (SAR_{1g}) for the occupational and public exposures cannot be exceeded 8 and 1.6 W/kg [1], respectively. After EM simulation is done and the steady-state fields are achieved using the discrete Fourier transform (DFT), the magnitudes of the averaged *E* field components are used for the calculation of the steady-state SAR distribution at each frequency of interest. The SAR is defined at a given location as:

$$SAR(i,j,k) = \frac{\sigma(i,j,k)}{2\rho(i,j,k)}\left(\left|E_x(i,j,k)\right|^2 + \left|E_y(i,j,k)\right|^2 + \left|E_z(i,j,k)\right|^2\right), \tag{2}$$

where $\sigma(i,j,k)$ and $\rho(i,j,k)$ are the electric conductivity and mass density [kg/m^3] of the tissue at a given location, respectively. In equation (2), an averaging of E fields in all directions is performed to obtain the corresponding values at the exact location of interest. For calculating the peak SAR_{1g} in the head, the IEEE standard C95.3-2002 is considered [24]. These SAR_{1g} values are considered as RF heat source in the temperature rise calculation.

D. Temperature rise calculation

After the SAR_{1g} distribution in the head is calculated and recorded, the temperature analysis with the use of bioheat equation [21] is performed in two steps. In the first step, the steady-state temperature distribution in the head is calculated by solving the bioheat equation with no RF heat source (SAR_{1g}=0). In the second step, the final temperature distribution is calculated by substituting the SAR_{1g} distribution into the bioheat equation. The difference between the final and steady-state temperature distribution provides the temperature rise distribution in the head.

The bioheat equation is given by:

$$\rho \cdot C \cdot \frac{\partial T}{\partial t} = K \cdot \nabla^2 T + \rho \cdot SAR_{1g} - B \cdot \left(T - T_b\right), \tag{3}$$

where T is the temperature of the tissue at time t, ρ is the mass density of the tissue [kg/m^3], C is the heat capacity of the tissue [J/(kg·°C)], K is the thermal conductivity of the tissue [J/(m·°C)], B is the blood perfusion rate [W/(m^3.°C)], and T_b is the blood temperature. The convective boundary condition [9] for the bioheat equation in (3) applied to the external and internal surface of the human head is expressed as:

$$K \cdot \frac{\partial T}{\partial n} = -h \cdot \left(T - T_{air}\right), \tag{4}$$

where T_{air} is the air temperature, n is the unit normal

vector to the skin surface or internal cavity, and h is the convection heat transfer coefficient [W/(m^2·^{o}C)]. The finite difference approximation of the bioheat equation in (3) and the convective boundary condition in (4) is given in [19]. The mass density and thermal parameters of the head tissues are given in [19]. The convection heat transfer coefficients (h) is set to 10.5 between the skin surface and external air and 50 between the internal cavity surface and internal air [5]. The air temperature (T_{air}) and initial head temperature (T_b) were set to 20 and 37 ^{o}C, respectively. In order to ensure the numerical stability, the temperature time-step (Δt) must satisfy the following criterion [9]:

$$\Delta t \le \frac{2\rho C d^2}{12K + Bd^2}. \quad (5)$$

III. NUMERICAL RESULTS

In the first part of this section, the maximum SAR_{1g} and temperature rise in the head are calculated at 1.5 GHz using the multiphysics model and traditional FDTD method. The obtained results are compared with the results obtained in [5-6] in order to prove the validity of the multiphysics model. In the second part of this section, the effects of frequency and incident angle of the RF fields on the SAR and temperature rise distributions in the head are investigated using the multiphysics model. Finally, in the last part of this section, the performance of the multiphysics model is presented. The computer being used in this paper has Intel® Core™ i7-4790 CPU and 16 GB DDR RAM. The program is written and compiled in 64-bit MATLAB version 8.2.0.701 (R2013b). The total number of cells used in the simulations is 14,007,552.

A. Comparison of results obtained using the multiphysics model and traditional FDTD method

In order to confirm the validity of the multiphysics model, the maximum temperature rise and SAR_{1g} values in the head calculated at 1.5 GHz using the multiphysics model are compared with those obtained using the traditional FDTD method and those reported in [5-6] for the occupational and public exposures. In this simulation, the human head with a cell size of 2 mm is illuminated by a θ polarized plane wave with the incident angles of θ^{inc}=90^o and ϕ^{inc}=90^o (from the front to rear of the head). The comparison in Table 1 shows that the results obtained using the multiphysics model agree very well with the results obtained using the traditional FDTD method. It is also realized that the maximum SAR_{1g} value in the head is reasonably in good agreement whereas the maximum temperature rise in the head is slightly different with those reported in [5-6]. The reason for the difference in the compared results is due to the use of different head model.

Table 1: Comparison of maximum SAR_{1g} and maximum temperature rise in the head at 1.5 GHz

Exposure Type	Methods	Max. SAR_{1g} (W/kg)	Max. Temp. Rise (°C)
Occupation RF Exposure	Multiphysics model	5.55	0.49
	Traditional FDTD	5.55	0.49
	Reported in [5]	**5.62**	**0.35**
Public RF Exposure	Multiphysics model	1.11	0.09
	Traditional FDTD	1.11	0.09
	Reported in [6]	**1.12**	**0.069**

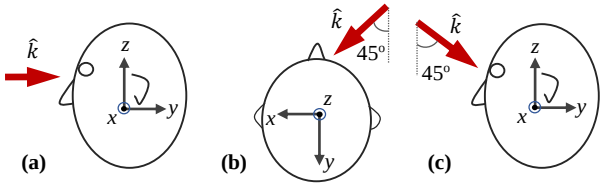

Fig. 1. (a) Front, (b) front-right, and (c) front-above.

B. Effect of frequencies and incident angles on the SAR and temperature rise distributions in the head

The temperature rise and SAR_{1g} distributions in the head due to the occupational RF field exposure are calculated using the multiphysics model at 5G frequencies below 6 GHz (3.4, 3.8, 4.4, and 4.9 GHz) in a single simulation. In order to excite the human head, a θ polarized plane wave is considered with three different incident angles: first is called front incident with the angles of θ^{inc}=90^o and ϕ^{inc}=90^o, second is called front-right incident with the angles of θ^{inc}=90^o and ϕ^{inc}=45^o, and third is called front-above incident with the angles of θ^{inc}=135^o and ϕ^{inc}=90^o, as shown in Fig. 1.

For the front incident, the SAR_{1g} and resulting temperature rise distributions in the x-y cross section of the head model at the listed frequencies are shown in Fig. 2. For the front-right and front-above incidence, the SAR_{1g} and resulting temperature rise distributions in the x-y cross section of the head model at the listed frequencies are shown in Figs. 3-4, respectively. It can be realized from the figures that SAR_{1g} distributions are correlated well with the temperature rise in the head. It can be seen from Fig. 3 that the SAR_{1g} and temperature rise values in the right eye are higher than those in the left eye because the nose prevents the RF fields from penetrating in the left eye. The electric conductivities of the tissues become larger as the frequency is increased, then the magnitude of EM waves in the head decreases exponentially. Therefore, the SAR_{1g} and resulting temperature rise values in the head decrease at higher frequencies.

The maximum SAR_{1g} value and temperature rise in the head at the listed frequencies are shown in Table 2 for front, front-right, and front-above incidence. It is realized that the maximum values of the SAR and temperature rise obtained from the front-above incident are smaller than those obtained from other two incidence. The maximum temperature rise and SAR_{1g} in the head are less than 1 ^{o}C and 8 W/kg for the occupational exposure, respectively.

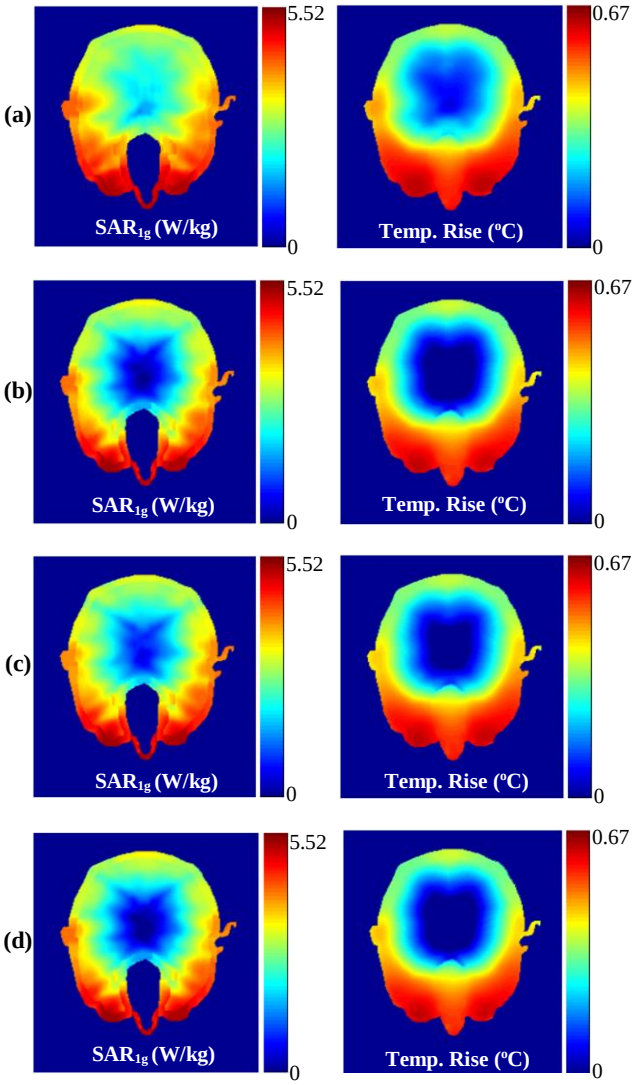

Fig. 2. SAR_{1g} and temperature rise distributions due to front incident at: (a) 3.4, (b) 3.8, (c) 4.4, and (d) 4.9 GHz.

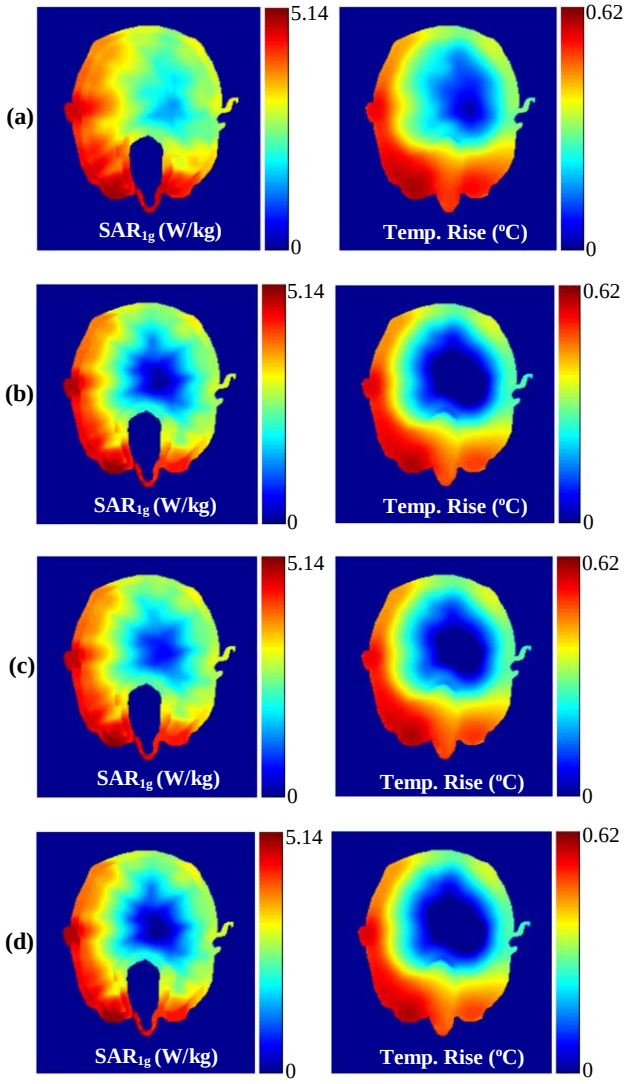

Fig. 3. SAR_{1g} and temperature rise distributions due to front-right incident at: (a) 3.4, (b) 3.8, (c) 4.4, and (d) 4.9 GHz.

The maximum temperature variation in the head at 3.4 GHz as a function of time is shown in Fig. 5 for the front, front-right, and front-above incidence. It can be seen from Fig. 5 that the temperature increases rapidly over the first 6 minutes, then temperature increase slows down, and the maximum (steady-state) temperature is reached after 30 minutes of exposure. The temperature rise due to the RF electromagnetic fields exposure is not significantly much to change the EM and thermal properties of the tissues.

Table 2: Maximum SAR_{1g} and temperature rise at listed frequencies for three different incidence

Freq.	**Max. SAR_{1g} (W/kg)**			**Max. Temperature Rise (°C)**		
(GHz)	Front	Front-right	Front-above	Front	Front-right	Front-above
3.4	5.52	5.14	2.98	0.67	0.62	0.37
3.8	4.01	3.66	2.99	0.56	0.45	0.31
4.4	3.33	4.08	3.16	0.45	0.49	0.31
4.9	3.24	3.65	2.82	0.44	0.43	0.31

C. Performance of multiphysics model

The SAR_{1g} and temperature rise values at the listed frequencies obtained using the multiphysics model in a single simulation are found to be exactly the same as those obtained using the traditional FDTD method using multiple simulations. The complexity of the traditional FDTD method [20] is less than that of the multiphysics model. However, the traditional FDTD method provides solutions at a single frequency in a single simulation because of frequency dependent of the biological tissues, whereas the multiphysics model can provide solutions at multiple frequencies using a single simulation. To show the performance of the multiphysics model, the relative percentage time saving between the multiphysics model and the traditional FDTD method is shown in Fig. 6 when the number of frequencies of interest is increased.

The relative percentage of CPU time saving between the multiphysics model and the traditional FDTD method is defined as:

$$t_{saving} = \left(\frac{t_{FDTD} - t_{multiphysics}}{t_{FDTD}} \right) \times 100\%, \qquad (6)$$

where $t_{multiphysics}$ and t_{FDTD} are the computation time of multiphysics model and the traditional FDTD method, respectively. It is realized that the multiphysics model is more efficient than the traditional FDTD method while obtaining solutions at more than one frequency. The solutions at frequencies above 20 GHz can be obtained using the multiphysics model once the three-term Debye coefficients of the tissues are determined using a numerical technique similar to that developed in [22].

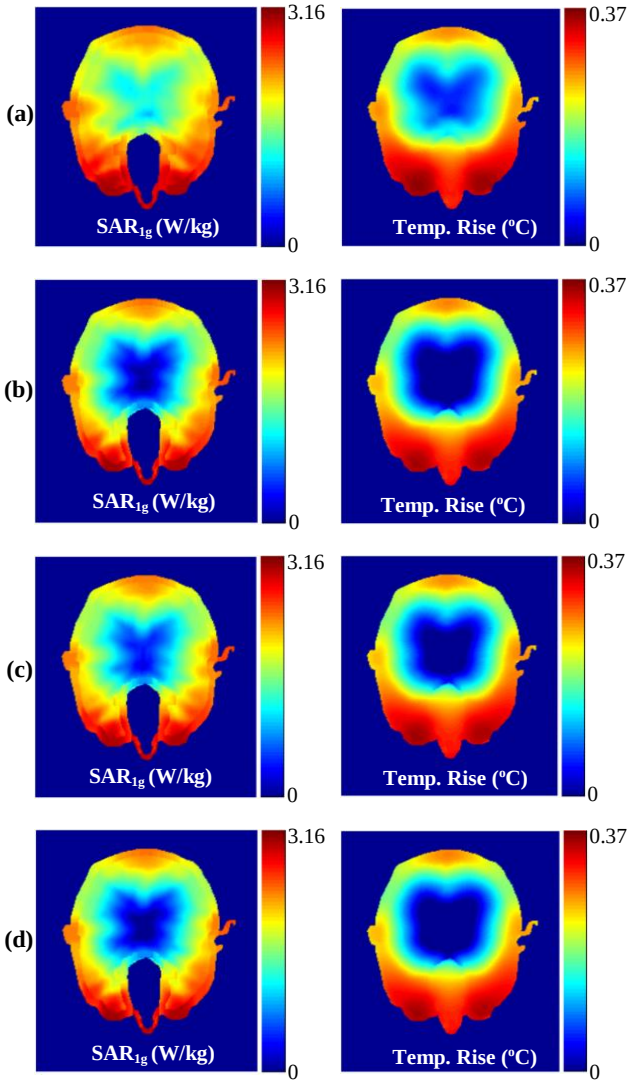

Fig. 4. SAR_{1g} and temperature rise distributions due to front-above incident at: (a) 3.4, (b) 3.8, (c) 4.4, and (d) 4.9 GHz.

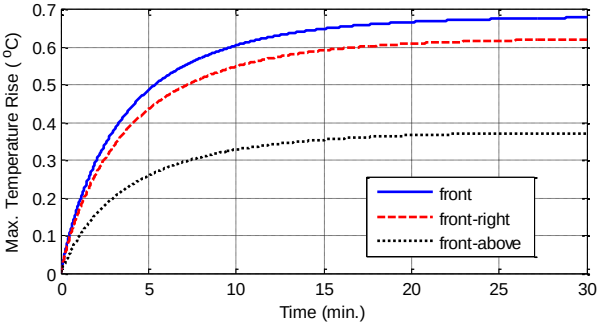

Fig. 5. Maximum temperature rise in the head at 3.4 GHz for front, front-right, and front-above incidence.

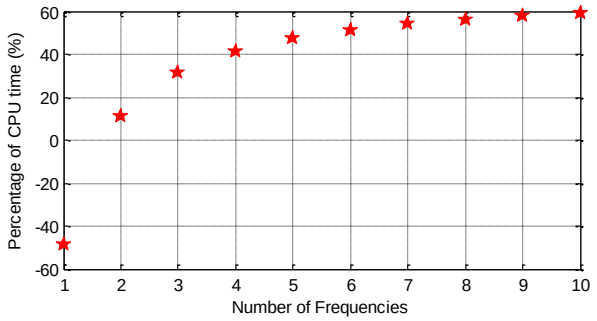

Fig. 6. Relative percentage of CPU time saving.

IV. CONCLUSION

The interaction between a dispersive human head and RF electromagnetic fields radiated by 5G base station is investigated using the multiphysics model at multiple frequencies in a single simulation. The SAR_{1g} and resulting temperature rise distributions in the head are calculated at 5G frequencies (3.4, 3.9, 4.4, and 4.9 GHz) in a single simulation with the use of multiphysics model. Numerical results show that the SAR_{1g} and temperature rise distributions in the human head are dependent on the frequency and incident angle of the RF fields. It is also realized that the maximum SAR_{1g} and temperature rise values occur in the eyes of the head. The multiphysics model provides remarkable saving in the computation time when the analysis is performed at more than one frequency.

REFERENCES

[1] Federal Communications Commission, "Evaluating compliance with FCC guidelines for human exposure to radio frequency electromagnetic fields," Rep., Washington, DC, Tech. Rep. OET Bull. 65, 1997.

[2] International Commission on Non-Ionizing Radiation Protection (ICNIRP), "Guidelines for limiting exposure to time-varying electric, magnetic,

and electromagnetic fields (up to 300 GHz)," *Health Phys.*, vol. 74, pp. 494-522, 1998.

[3] IEEE C95.1. IEEE standard for safety levels with respect to human exposure to radio frequency electromagnetic fields, 3 kHz to 300 GHz, IEEE Standard C95.1-2005, 2006.

[4] Y. Lu, J. Ying, T-K. Tan, and K. Arichandran, "Electromagnetic and thermal simulations of 3-D human head model under RF radiation by using the FDTD and FD approaches," *IEEE Transactions on Magnetics*, vol. 32, no. 3, pp. 1653-1656, 1996.

[5] O. Fujiwara, M. Yano, and J. Wang, "FDTD computation of temperature rise inside a realistic head model for 1.5-GHz microwave exposure," *Electron. Comm. Jpn. Pt. I*, vol. 82, no. 3, pp. 240-247, 1999.

[6] M. Yano, J. Wang, and O. Fujiwara, "FDTD computation of temperature rise in a realistic head models simulating adult and infant for 1.5-GHz microwave exposure," *Electron. Comm. Jpn. Pt. I*, vol. 84, no. 4, pp. 57-66, 2001.

[7] I. Laakso, "Assessment of the computational uncertainty of temperature rise and SAR in the eyes and brain under far-field exposure from 1 to 10 GHz," *Physics in Medicine and Biology*, vol. 54, pp. 3393-3404, 2009.

[8] S. Kodera, J. Gomez-Tames, and A. Hirata, "Temperature elevation in the human brain and skin with thermoregulation during exposure to RF energy," *BioMedical Engineering Online*, vol. 17, no. 1, pp. 1-17, Jan. 2018.

[9] J. Wang and O. Fujiwara, "FDTD computation of temperature rise in the human head for portable telephones," *IEEE Trans. Microwave Theory Tech.*, vol. 47, pp. 1528-1534, Aug. 1999.

[10] P. Bernardi, M. Cavagnaro, S. Pisa, and E. Piuzzi, "Specific absorption rate and temperature increases in the head of a cellular-phone user," *IEEE Trans. Microwave Theory Tech.*, vol. 48, pp. 1118-1126, July 2000.

[11] P. Bernardi, M. Cavagnaro, S. Pisa, and E. Piuzzi, "Power absorption and temperature elevations induced in the human head by a dual-band monopole-helix antenna phone," *IEEE Trans. Microwave Theory Tech.*, vol. 49, no. 12, pp. 2539-2546, Dec. 2001.

[12] A. Hirata, M. Morita, and T. Shiozawa, "Temperature increase in the human head due to a dipole antenna at microwave frequencies," *IEEE Trans. Electromag. Compat.*, vol. 45, no. 1, pp. 109-116, Feb. 2003.

[13] A. Hirata, G. Ushio, and T. Shiozawa, "Calculation of temperature rises in the human eye exposed to EM waves in the ISM frequency bands," *IEICE Trans. Commun.*, vol. E83-B, no. 3, pp. 541-548, Mar. 2000.

[14] A. Hirata, S. Matsuyama, and T. Shiozawa, "Temperature rise in the human eye exposed to EM waves in the frequency range 0.6-6 GHz," *IEEE Trans. Electromag. Compat.*, vol. 42, no. 4, pp. 386-393, Nov. 2000.

[15] A. Hirata, H. Watanabe, and T. Shiozawa, "SAR and temperature increase in the human eye induced by obliquely incident plane waves," *IEEE Trans. Electromag. Compat.*, vol. 44, no. 4, pp. 592-594, Nov. 2002.

[16] A. Hirata, "Temperature increase in human eyes due to near-field and far-field exposures at 900 MHz, 1.5 GHz, and 1.9 GHz," *IEEE Trans. Electromag. Compat.*, vol. 47, no. 1, pp. 68-76, Feb. 2005.

[17] P. Bernardi, M. Cavagnaro, S. Pisa, and E. Piuzzi, "SAR distribution and temperature increase in an anatomical model of the human eye exposed to the field radiated by the user antenna in a wireless LAN," *IEEE Trans. Microwave Theory Tech.*, vol. 46, no. 12, pp. 2074-2082, Dec. 1998.

[18] C. Buccella, V. D. Santis, and M. Feliziani, "Prediction of temperature increase in human eyes due to RF sources," *IEEE Trans. Electromag. Compat.*, vol. 49, no. 4, pp. 825-833, Nov. 2007.

[19] F. Kaburcuk and A. Z. Elsherbeni, "Temperature rise and SAR distribution at wide range of frequencies in a human head due to an antenna radiation," *ACES Journal*, vol. 33, no. 4, pp. 367-372, April 2018.

[20] A. Z. Elsherbeni and V. Demir, *The Finite-Difference Time-Domain Method for Electromagnetics with MATLAB Simulations*, second edition, ACES Series on Computational Electromagnetics and Engineering, SciTech Publishing, an Imprint of IET, Edison, NJ, 2016.

[21] H. H. Pennes, "Analysis of tissue and arterial blood temperature in resting forearm," *J. Appl. Physiol.*, vol. 1, pp. 93-122, 1948.

[22] M. A. Eleiwa and A. Z. Elsherbeni, "Debye constants for biological tissues from 30 Hz to 20 GHz," *ACES Journal*, vol. 16, no. 3, pp. 202-213, Nov. 2001.

[23] http://noodle.med.yale.edu/zubal/ [Online website 2017].

[24] *IEEE Recommended Practice for Measurements and Computations of Radio Frequency Electromagnetic Fields With Respect to Human Exposure to Such Fields, 100 kHz-300 GHz*, IEEE Standard C95.3-2002, Annex E, 2002.

Fatih Kaburcuk received both the M.Sc. and Ph.D. degrees in Electrical Engineering from Syracuse University, Syracuse, New York, USA, in 2011 and 2014, respectively. He was a visiting research scholar in the Electrical Engineering Department at Colorado School of Mines in 2014. Currently, Kaburcuk is an Assistant Professor at the Department of Electrical and Electronics Engineering at Erzurum Technical University, Turkey. His research interest includes numerical methods in electromagnetics, bioelectromagnetic, and microwave systems.

Atef Z. Elsherbeni received his Ph.D. degree in Electrical Engineering from Manitoba University, Winnipeg, Manitoba, Canada, in 1987. Elsherbeni was with the University of Mississippi from 1987 to 2013. He was a Finland Distinguished Professor from 2009 to 2011. He joined the Electrical Engineering and Computer Science Department at Colorado School of Mines in August 2013 as the Dobelman Distinguished Chair Professor. His research interest includes the scattering and diffraction of EM waves, finite-difference time-domain analysis of antennas and microwave devices, field visualization and software development for EM education, interactions of electromagnetic waves with the human body, RFID and sensor integrated FRID systems, reflector and printed antennas and antenna arrays, and measurement of antenna characteristics and material properties. His academic achievements includes: Funded Research Grants with a total amount of $11,413,903, 13 books, 29 book chapters, 171 journal publications, 15 developed software packages, 56 (35 M.S. and 21 Ph.D.) graduate students advised, 40 invited presentations, 221 proceedings publications, 174 conference abstracts, 74 technical reports, 35 short courses offered, 43 invited talks. Elsherbeni is a Fellow Member of IEEE and ACES. He is the Editor-in-Chief for ACES Journal. He was the General Chair for the 2014 APS-URSI Symposium and was the President of ACES Society from 2013 to 2015.